Prostaglandin E_2 deficiency uncovers a dominant role for thromboxane A_2 in house dust mite-induced allergic pulmonary inflammation

Tao Liu[a,b], Tanya M. Laidlaw[a,b,c], Chunli Feng[a,b], Wei Xing[a,b], Shiliang Shen[a,b], Ginger L. Milne[d], and Joshua A. Boyce[a,b,c,1]

Departments of [a]Medicine and [c]Pediatrics, Harvard Medical School, Boston, MA 02115; [b]Division of Rheumatology, Immunology, and Allergy, Jeff and Penny Vinik Center for Allergic Disease Research, Brigham and Women's Hospital, Boston, MA 02115; and [d]Department of Pharmacology, Vanderbilt University, Nashville, TN 37232

Edited* by K. Frank Austen, Brigham and Women's Hospital, Boston, MA, and approved June 20, 2012 (received for review May 10, 2012)

Prostaglandin E_2 (PGE_2) is an abundant lipid inflammatory mediator with potent but incompletely understood anti-inflammatory actions in the lung. Deficient PGE_2 generation in the lung predisposes to airway hyperresponsiveness and aspirin intolerance in asthmatic individuals. PGE_2-deficient *ptges*$^{-/-}$ mice develop exaggerated pulmonary eosinophilia and pulmonary arteriolar smooth-muscle hyperplasia compared with PGE_2-sufficient controls when challenged intranasally with a house dust mite extract. We now demonstrate that both pulmonary eosinophilia and vascular remodeling in the setting of PGE_2 deficiency depend on thromboxane A_2 and signaling through the T prostanoid (TP) receptor. Deletion of TP receptors from *ptges*$^{-/-}$ mice reduces inflammation, vascular remodeling, cytokine generation, and airway reactivity to wild-type levels, with contributions from TP receptors localized to both hematopoietic cells and tissue. TP receptor signaling ex vivo is controlled heterologously by E prostanoid $(EP)_1$ and EP_2 receptor-dependent signaling pathways coupling to protein kinases C and A, respectively. TP-dependent up-regulation of intracellular adhesion molecule-1 expression is essential for the effects of PGE_2 deficiency. Thus, PGE_2 controls the strength of TP receptor signaling as a major bronchoprotective mechanism, carrying implications for the pathobiology and therapy of asthma.

cyclooxygenase | EP receptors

Prostaglandins (PGs) derive from the metabolism of arachidonic acid by cyclooxygenase (COX)-1 and COX-2 (1). COX-derived PGH_2 is converted to one of five PGs [PGD_2, PGE_2, $PGF_2\alpha$, PGI_2, or thromboxane A_2 (TXA_2)] by distinct terminal synthases. Specific G protein-coupled receptors (2) mediate the effects of PGs in vivo, including roles in regulation of vascular tone, hemostasis, hematopoiesis, epithelial cell turnover, cancer, and inflammation (1). Although COX inhibitors control inflammatory pain (3) and may prevent vascular disease and certain cancers (1), these reagents can also interfere with the production of PGs needed for homeostatic functions and cause unwanted side effects (1, 4).

PGE_2 is one of the most functionally versatile PGs. Three terminal synthases can convert PGH_2 to PGE_2 (5–7). Of these, microsomal PGE_2 synthase (mPGES)-1 is the dominant enzyme responsible for converting COX-2–derived PGH_2 to PGE_2 during inflammation (8). Four E prostanoid (EP) receptors (9) mediate the effects of PGE_2. PGE_2 is pathogenetic in models of autoimmune diseases (10) and inflammatory arthritis (8), but is bronchoprotective (11) and anti-inflammatory (12, 13) in certain models of allergic lung disease. In patients with atopic asthma, inhalation of PGE_2 blocks bronchoconstriction in response to challenge with inhaled specific allergen (14) and attenuates the recruitment of eosinophils and basophils to the airway. Reduced PGE_2 levels in the setting of sputum eosinophilia correlate with airway hyperresponsiveness (AHR) (15), a cardinal feature of asthma. Aspirin-exacerbated respiratory disease (AERD), a severe variant of asthma, is associated with deficient COX-2–derived PGE_2 production (16–19) and reduced expression of the EP_2 receptor (20, 21), as well as marked tissue eosinophilia and bronchoconstrictive responses to the administration of nonselective COX inhibitors. These findings suggest potential therapeutic applications of PGE_2 in asthma and AERD if the mechanisms responsible for the homeostatic functions of PGE_2 in asthma can be fully defined.

An extract (*Df*) of the house dust mite *Dermatophagoides farinae* contains clinically relevant protease allergens, as well as adjuvants (glycans, endotoxin) that elicit sensitization through the airway mucosa, resulting in eosinophilic airway inflammation and a mixed T helper (Th)2, Th1, and Th17 pulmonary immune response (22). PGE_2-deficient mice with a targeted deletion in the gene encoding mPGES-1 (*ptges*$^{-/-}$ mice) develop increased bronchovascular eosinophilia compared with WT C57BL/6 controls when challenged intranasally with a low dose (3 μg) of *Df* (12), revealing a bronchoprotective effect of endogenous PGE_2. This effect is restored by administration of agonists of the EP_1, EP_2, and EP_3 receptors. *Df*-challenged *ptges*$^{-/-}$ mice also develop extensive remodeling of the small- to medium-sized pulmonary arterioles (12), a feature observed with sustained pulmonary Th2 responses in WT mice induced by inhaled allergens (23). TXA_2, a platelet-derived PG, activates endothelial-dependent leukocyte recruitment (24), causes constriction and proliferation of pulmonary vascular smooth muscle (25, 26), and amplifies airway reactivity to methacholine (MCh) in humans (27). Because of its prominent pulmonary vascular and airway effects, we speculated that TXA_2 might mediate the pathologic effects of PGE_2 deficiency in the lung. We now demonstrate that virtually all functional and immunologic perturbations resulting from PGE_2 deficiency in *Df*-treated mice are prevented by the deletion of *tpr* encoding the T prostanoid (TP)α and TPβ receptors for TXA_2. PGE_2 mediates bronchoprotection in part by controlling TXA_2 effector pathways, suggesting that pharmacologic blockade of TP receptors may prove helpful for the treatment of asthma variants in which local PGE_2-mediated homeostasis is deficient.

Results and Discussion

Dust Mite-Mediated Bronchovascular Inflammation and Vascular Remodeling in *ptges*$^{-/-}$ Mice Depends on TP Receptor Signaling. Because the vascular remodeling observed in *Df*-challenged

Author contributions: J.A.B. designed research; T.L., T.M.L., C.F., W.X., and S.S. performed research; T.M.L. and G.L.M. contributed new reagents/analytic tools; T.L., W.X., and S.S. analyzed data; and T.M.L. and J.A.B. wrote the paper.

The authors declare no conflict of interest.

*This Direct Submission article had a prearranged editor.

[1]To whom correspondence should be addressed. E-mail: Jboyce@rics.bwh.harvard.edu.

This article contains supporting information online at www.pnas.org/lookup/suppl/doi:10.1073/pnas.1207816109/-/DCSupplemental.

ptges$^{-/-}$ mice suggested a potential contribution from TP receptors, we eliminated TP receptors in *ptges*$^{-/-}$ mice by mating them with *tpr*$^{-/-}$ C57BL/6 mice (28). As expected, the intranasal administration of *Df* (3 μg) elicited mild inflammation in WT C57BL/6 mice, and severe inflammation in *ptges*$^{-/-}$ mice (12). *Ptges*$^{-/-}$ mice demonstrated higher total bronchoalveolar lavage (BAL) fluid cell counts, eosinophils, macrophages, lymphocytes, and neutrophils relative to WT controls (Fig. 1*A*). *Df*-challenged *ptges*$^{-/-}$ mice had slightly more Periodic acid-Schiff (PAS)-staining goblet cells and cellular infiltration of their bronchovascular structures than did the WT controls (Fig. 1*B*, *Top*, as shown in Fig. 1*C*). Deletion of *tpr* from the *ptges*$^{-/-}$ mice reduced all of these features to levels indistinguishable from or below those of WT controls (Fig. 1). Findings in WT controls did not differ from those in the *tpr*$^{-/-}$ single KO mice (Fig. 1), although single KO mice showed reduced eosinophilic inflammation in experiments where the dose of *Df* was increased to 10 μg (Fig. S1).

Pulmonary arteriolar remodeling is not a feature of asthma in humans, but develops in sensitized WT mice treated with long-term or high-dose allergen (23, 29). In our previous study (12), *ptges*$^{-/-}$ mice developed significant increases in the numbers of α-smooth muscle actin (α-SMA)$^{+}$ cells and the thickness of the α-SMA^{+} cell layer in lung sections at doses of dust mite allergen ∼10-fold lower than those used to elicit this response in WT mice in other reports (29). Administration of selective EP_1, EP_2 (especially), and EP_3 agonists protected *ptges*$^{-/-}$ mice from remodeling (12). In the present study, the *Df*-induced vasculopathy in the *ptges*$^{-/-}$ mice was completely eliminated by the introduction of the *tpr*$^{-/-}$ allele (Fig. 2). Treatment of the *ptges*$^{-/-}$ mice with intraperitoneal injections of the selective TP receptor antagonist SQ 29,548 each day (2 mg/kg of body weight) during the period of *Df* challenge reduced total BAL cell and eosinophil counts (Fig. S2*A*), bronchovascular inflammation, goblet cell metaplasia, and vascular remodeling (Fig. S2*B*). These data strongly indicate that TP receptors are dominant effectors of pulmonary inflammation and its pathophysiologic consequences when PGE_2 is depleted.

Deletion of TP Receptors Eliminates the Increment in Airway Reactivity Observed in *Df*-Challenged PGE_2-Deficient Mice. AHR to MCh is a feature of asthma that is potentiated after allergen challenge of atopic humans. Although inhaled PGE_2 blocks allergen-induced potentiation of AHR (14), inhaled TXA_2 causes bronchoconstriction and potentiates AHR (27). Although exogenously administered PGE_2 and TXA_2, respectively, dampen and potentiate airway reactivity to MCh in mice (11, 30), the roles of endogenous PGs in controlling allergen-induced AHR are less clear. Indeed, a recent study reported that *ptges*$^{-/-}$ mice showed reduced MCh reactivity compared with WT controls in a model of pulmonary disease where mice were immunized systemically to ovalbumin (31). In contrast to that study, *Df*-challenged *ptges*$^{-/-}$ mice displayed greater AHR than did *Df*-challenged WT mice over the entire range of MCh doses (6.25–100 mg/mL). Deletion of the *tpr* allele from the *ptges*$^{-/-}$ mice restored MCh reactivity following *Df* challenge to WT levels (Fig. 3). Thus, endogenous PGE_2 is strongly bronchoprotective against AHR in our model, and does so at least in part by suppressing the pathogenetic

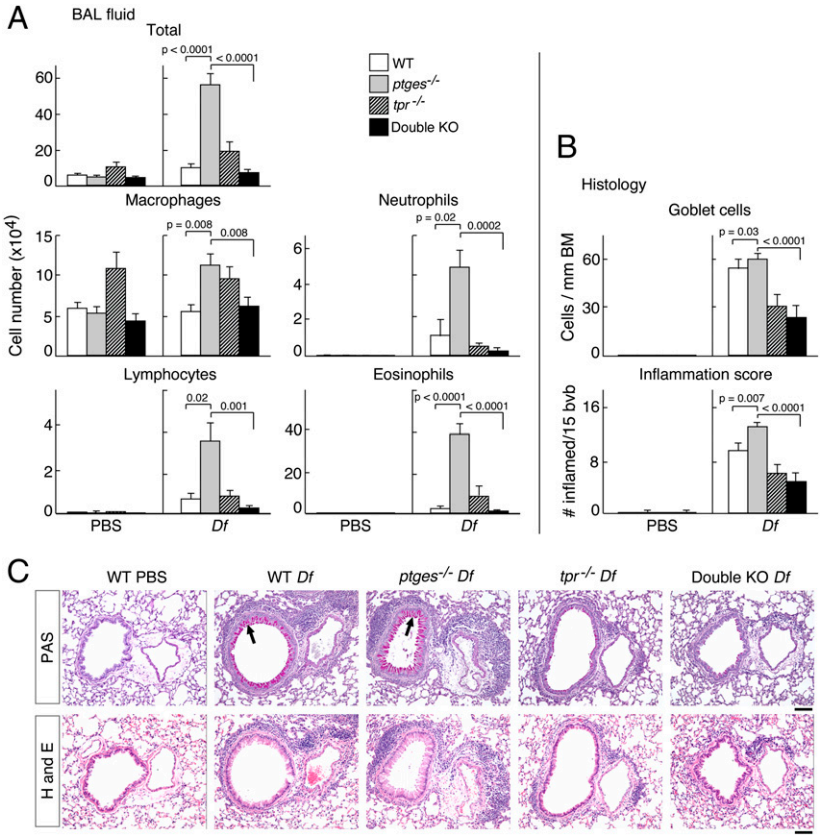

Fig. 1. Deletion of TP receptors eliminates the potentiation of pulmonary inflammation in PGE_2-deficient mice. Mice were challenged intranasally with either *Df* (3 μg) or saline on days 0, 3, 7, 10, 14, and 17, and were killed on day 18. (*A*) The numbers of total cells, macrophages, neutrophils, lymphocytes, and eosinophils recovered from the BAL fluid of saline-challenged and *Df*-challenged mice of the indicated genotypes are displayed. (*B*) Quantitative analysis of goblet cell numbers (*Upper*, based on PAS staining) and cellular infiltration of bronchovascular bundles (*Lower*, based on H&E staining). (*C*) Representative samples of lungs stained with PAS (*Upper*) and H&E (*Lower*) showing bronchovascular bundles for each genotype. Results in *A* and *B* are mean ± SD from 15 to 20 mice per group from four different experiments. BM, basement membrane. (Scale bars, 100 μm.)

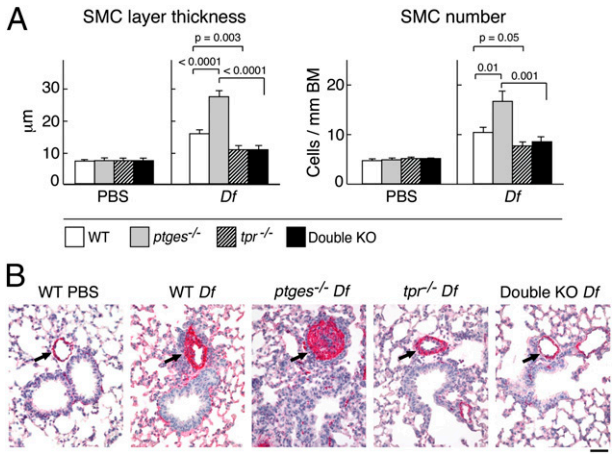

Fig. 2. TP receptors mediate *Df*-induced remodeling of pulmonary arterioles in *ptges*$^{-/-}$ mice. Paraffin-embedded lungs from the saline- or *Df*-challenged mice were stained with an Ab for α-SMA and counterstained with H&E. (*A*) Thickness of α-SMA–staining layer (*Left*) and numbers of α-SMA^{+} cells per millimeter of basement membrane (BM) (*Right*) in the lungs of the indicated genotypes. (*B*) Representative images for each genotype are shown. Arrows show arterioles. Data in *A* are mean ± SD from 15 to 20 mice per group from four separate experiments. (Scale bar, 100 μm.)

contribution from TP receptors. *Tpr* deletion also slightly increased basal reactivity to the highest doses of MCh in naive, PGE_2-sufficient mice (Fig. 3).

Deletion of TP Receptor Signaling Attenuates Th2-Type Recall Responses to *Df*. Allergen-induced eosinophilic inflammation, pulmonary vascular remodeling, and AHR in mice are all characteristic signatures of Th2-type cytokines (23, 32). *Df* elicits a mixed Th1, Th2, and Th17-type pulmonary immune response in mice based on cytokine profiles of restimulated lung-draining parabronchial lymph node (PLN) cells. Because both PGE_2 and TXA_2 can exert complex effects on T cells depending on the model studied (33, 34), we measured cytokines generated by *Df*-restimulated PLN cells from each strain. The cells from *Df*-treated *ptges*$^{-/-}$ mice generated more IL-4, IL-5, IL-13, and IL-17A than did the cells from WT animals, but produced less IFN-γ (Fig. S3). This finding is consistent with previous reports that PGE_2 promotes IFN-γ production in a Th1-dependent model of contact hypersensitivity (10). Because IFN-γ counteracts Th2 cell development, the lower level of IFN-γ generated by the *ptges*$^{-/-}$ PLN cells could amplify Th2 cytokine production occurring in our model. Deletion of the *tpr* allele reduced the levels of Th2 cytokines in both PGE_2-deficient and -sufficient genetic backgrounds (Fig. S3), and also reduced the levels of serum IgE and specific IgG1 (Fig. S4). Treatment with SQ 29,548 also reduced Th2 cytokine generation, although this was significant only for the PLNs from the *ptges*$^{-/-}$ mice (Fig. S2*C*). Thus, the pathologic and physiologic features of our model that are enhanced and abrogated by the absences of mPGES-1 and TP receptors could in part reflect the influences of PGE_2 and TXA_2, respectively, on cytokine production by T cells. The reduced levels of allergen-specific IgE and IgG1 could explain some of the protective effects of TP receptor deletion.

Absence of PGE_2 Does Not Increase TP Receptor-Dependent Pathology by Enhancing TXA_2 Formation. COX-2 and mPGES-1 ensure increased PGE_2 production with inflammation (35). Deletion of mPGES-1 can therefore alter the synthesis of other PGs through shunting of the COX-2–derived PGH_2 to other terminal synthases (36). We monitored the generation of all PGs by the cells of enzymatically dispersed lung cells from all strains. *Df* challenge induced a marked (~threefold) increase in PGE_2 generation by the lung cells of WT mice that were incubated ex vivo with arachidonic acid (50 μM), and increased the productions of $PGF_2\alpha$, PGI_2, PGD_2, and TXA_2 more modestly (Fig. S5). Consistent with our previous study (12), the deletion of *ptges* impaired the conversion of arachidonic acid to PGE_2 by the lung cells from *Df*-challenged mice, without altering conversion to other PGs (Fig. S5), but the deletion of TP receptors had no effect.

Because TXA_2 synthesis was not enhanced in the absence of mPGES-1, we suspected that the amplification of TP receptor-dependent contributions in this strain reflected deficient cross-regulation of TP receptor signaling by EP receptors. TP receptors in the lung are constitutively serine-phosphorylated by other receptors that maintain cAMP-dependent PKA activity, limiting the strength of TP receptor signaling (37, 38). TP receptors can also be phosphorylated and desensitized by PKC (38). As noted above, EP_1, EP_2, and EP_3 agonists all protect *ptges*$^{-/-}$ mice from vascular remodeling (12), and the EP_2 agonist also blocked bronchovascular inflammation and BAL fluid eosinophilia. Narumiya and colleagues showed a homeostatic role for EP_3 receptor signaling in a model of ovalbumin-induced airway disease (39). EP_2 and EP_4 receptors activate PKA (9), whereas EP_1 and EP_3 receptors can activate PKC (40, 41). We studied cross-regulation ex vivo in platelets and human umbilical vein endothelial cells (HUVEC), both of which express TP (42, 43) and EP receptors (42). The TP receptor-selective agonist U-46619 dose-dependently induced CD62P expression by platelets (Fig. 4 *A* and *B*). The platelets from *tpr*$^{-/-}$ mice showed no response to U-46619 (Fig. 5*B*). Pretreatment with an EP_1 receptor agonist (DI-004) suppressed TP-dependent induction of CD62P (Fig. 4*C*), whereas agonists of EP_2 (AE1-259-01), EP_3 (AE-248), and EP_4 receptors showed no effect below 10 μM. The effect of the EP_1 agonist was reversed by treatment of the samples with the PKC inhibitors Go6976 and Calphostin C (Fig. 4*D*). U-46619 induced

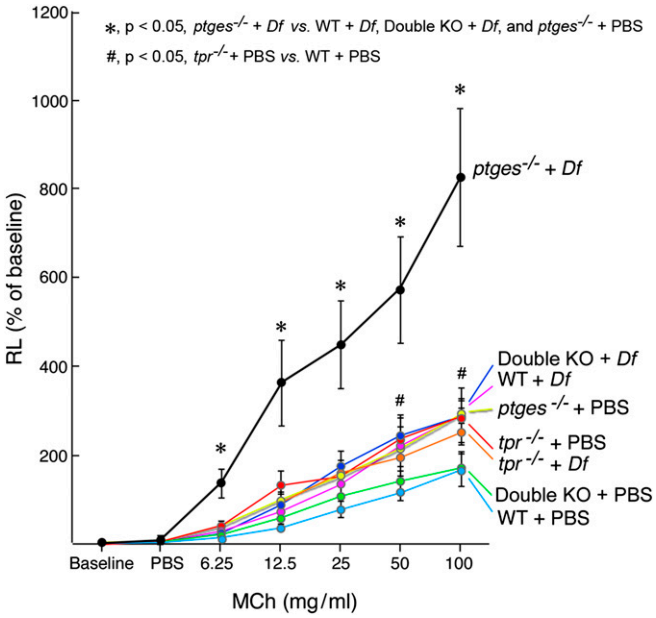

Fig. 3. Amplification of MCh reactivity in *Df*-challenged *ptges*$^{-/-}$ mice is TP receptor-dependent. Saline- or *Df*-challenged mice of the indicated genotypes were anesthetized and mechanically ventilated. Airway resistance was monitored during incremental inhalation challenge with MCh. Data are from 10 mice per group from two separate experiments. $^{*}P < 0.05$ vs. *Df*-treated WT group, *tpr*$^{-/-}$, and DKO groups. $^{\#}P < 0.05$ PBS-treated *tpr*$^{-/-}$ group vs. PBS-treated WT group.

IMMUNOLOGY

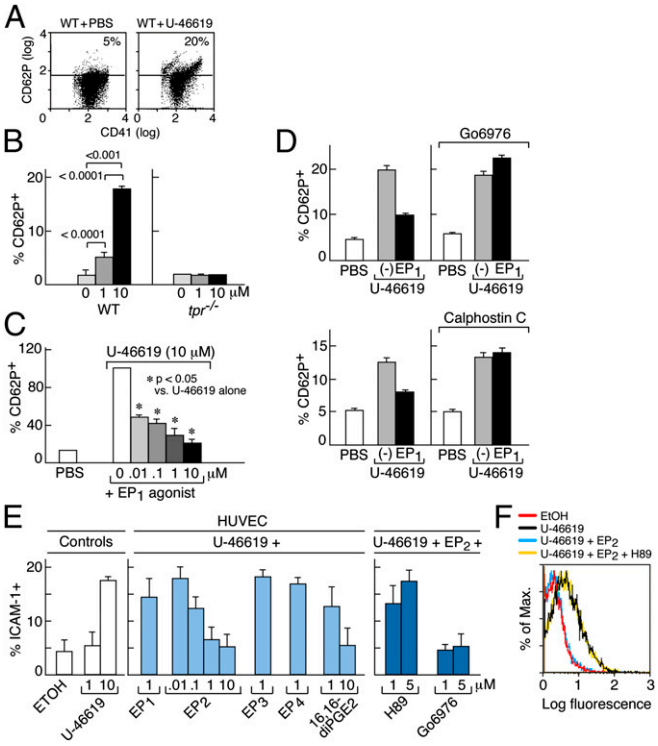

Fig. 4. EP_1 and EP_2 receptors control TP receptor signaling in platelets and endothelial cells, respectively. (*A*) Cytofluorographic detection of CD62P expression by platelets identified in whole blood after 15 min of stimulation with or without the selective TP receptor agonist U-46619 (10 μM). (*B*) Effects of various doses of U-46619 on CD62P expression by platelets in the blood of WT or $tpr^{-/-}$ mice. (*C*) Effect of various concentrations of the EP_1 receptor agonist DI-004 on TP receptor-mediated CD62P expression by blood platelets. (*D*) Effect of the PKC inhibitors Go6976 and Calphostin C on the suppression of TP-induced platelet CD62P expression by DI-004. Results in *B–D* are the mean ± SD from three separate experiments, with the induction of CD62P induced by U-46619 alone (10 μM) set at 100% for each experiment in *C*. (*E*) Effects of various EP receptor agonists on the induced expression of ICAM-1 by HUVEC cells stimulated with U-46619. The PKA inhibitor H89 was added to the indicated samples that were stimulated with U-46619 (10 μM) in the presence of the maximally effective dose (1 μM) of the EP_2 receptor agonist AE1-259–01. Data are mean ± range from two separate experiments. (*F*) A representative histogram from one of the two experiments is shown.

the expression of intercellular adhesion molecule (ICAM)-1 by HUVEC (Fig. 4 *E* and *F*). This induction was blocked by pretreatment with AE1-259–01 (0.1–10 μM) or the stable PGE_2 analog 16, 16-diPGE_2 (10 μM), but not with the other EP receptor selective agonists (Fig. 4 *E* and *F*). The EP_2 receptor-dependent blockade of ICAM-1 induction was reversed by the PKA inhibitor H89 (Fig. 4 *E* and *F*) but not by the PKC inhibitor Go6976 (Fig. 4*E*). Thus, TP receptor signaling on both hematopoietic and nonhematopoietic cells can be desensitized by EP_1 and EP_2 receptors through respective PKC- and PKA-dependent signaling pathways, consistent with the hypothesis that PGE_2 controls allergic pulmonary inflammation by maintaining heterologous desensitization of TP receptors.

TP Receptors Expressed by both Resident and Hematopoietic Cells Contribute to the Enhanced Pulmonary Response to Allergen in the Setting of PGE_2 Deficiency. To determine the extent to which TP receptors on hematopoietic cells and on resident tissue cells were important in our model, we generated chimeric $ptges^{-/-}$ mice lacking TP receptors on nonbone marrow-derived cells by transferring $ptges^{-/-}$ bone marrow into lethally irradiated double-KO mice. We also generated chimeric $ptges^{-/-}$ mice lacking TP receptors on bone marrow-derived cells by transferring double-KO bone marrow into irradiated $ptges^{-/-}$ mice. After 10 wk, the chimeric mice were challenged with either *Df* or saline. Control $ptges^{-/-}$ mice that were reconstituted with $ptges^{-/-}$ bone marrow developed *Df*-induced increases in total BAL fluid cell numbers, eosinophils, bronchovascular cellular infiltrates, and goblet cell metaplasia in response to *Df*. In contrast, double-KO mice reconstituted with double-KO bone marrow showed little response to *Df* challenge on all parameters (Fig. S6 *A–D*). Mice lacking TP receptors only on the hematopoietic compartment and mice lacking TP receptors only on the tissue compartment demonstrated *Df*-induced BAL fluid eosinophilia, bronchovascular inflammation, and PLN cytokine production that were intermediate between the $ptges^{-/-}$ and double-KO mice reconstituted with marrow from their corresponding respective identical littermates (Fig. S6). Peripheral blood cell counts were similar among the various groups (WBC counts ranging from 2.15 ± 0.43 to 3.07 ± 1.01 × 10^3 cells/μL, mean ± SD) and no different from the nonirradiated age-matched WT mice (2.77 ± 0.55 × 10^3 cells/μL). Thus, the functions of TP receptors on hematopoietic cells and nonhematopoietic cells are synergistic in this model, potentially reflecting the contributions of TP receptors to platelet-dependent priming of granulocyte adhesiveness (24, 44, 45) and enhancement of endothelial adhesion molecule expression (24), respectively. Both of these contributions may be held in check by PGE_2.

PGE_2 Deficiency Augments ICAM-1–Dependent Pulmonary Leukocyte Recruitment in Vivo. We next sought to directly determine whether TP receptors regulated leukocyte recruitment to the lung in the setting of PGE_2 deficiency by controlling the expression of ICAM-1. Double immunofluorescent staining with anti–ICAM-1 and anti–α-SMA (to identify the bronchovascular structures) revealed ICAM-1 staining in the WT and $ptges^{-/-}$ strains that tended to be more intense after challenges with *Df* (Fig. 5*A*, green fluorescence). Confocal images of lung double-stained with Abs against ICAM-1 and platelet endothelial adhesion molecule-1 (PECAM-1) revealed strong ICAM-1 signals on the PECAM-1^- alveolar epithelium, with additional colocalization to PECAM-1^+ endothelial cells (Fig. 5*B*). *Df* treatment strongly up-regulated ICAM-1 protein expression in the lungs of WT mice, and more strongly in the $ptges^{-/-}$ mice (Fig. 5*C*). Remarkably, *Df* treatment failed to up-regulate ICAM-1 protein in the lungs of $tpr^{-/-}$ and double-KO mice (Fig. 5*C*).

To determine whether the TP receptor-driven ICAM-1 expression observed in the $ptges^{-/-}$ mice accounted for the pathologic features observed in this strain, we treated WT and $ptges^{-/-}$ mice with intraperitoneal injections of blocking anti–ICAM-1 Abs or isotype controls during the period of *Df* challenge. ICAM-1 blockade markedly decreased the numbers of total cells and eosinophils in the BAL fluids from the $ptges^{-/-}$ mice and in the WT controls (Fig. S7*A*), and also reduced the bronchovascular inflammation, goblet cell metaplasia, and arteriolar remodeling (Fig. S7*B*, as shown in Fig. S7*C*). Anti–ICAM-1 treatment reduced the numbers of cells recovered from the PLNs of both strains of mice, and reduced the levels of IL-4, IL-5, and IL-13, but not IL-17A generated by the cells from both strains (Fig. S8). Thus, EP and TP receptor signaling pathways respectively dampen and induce ICAM-1 expression in the lung, controlling susceptibility to the pathologic and physiologic changes resulting from *Df*. The lack of PGE_2 likely dysregulates the control of TP receptor-dependent ICAM-1 expression as a major phenotypic component of the $ptges^{-/-}$ strain.

Our study suggests that the long recognized homeostatic function of PGE_2 in allergic pulmonary inflammation (12–14) and airway reactivity (15, 46) involves cross-regulation of TP receptor function. EP receptors "fine-tune" the strength of signaling through TP receptors by activating PKA and PKC.

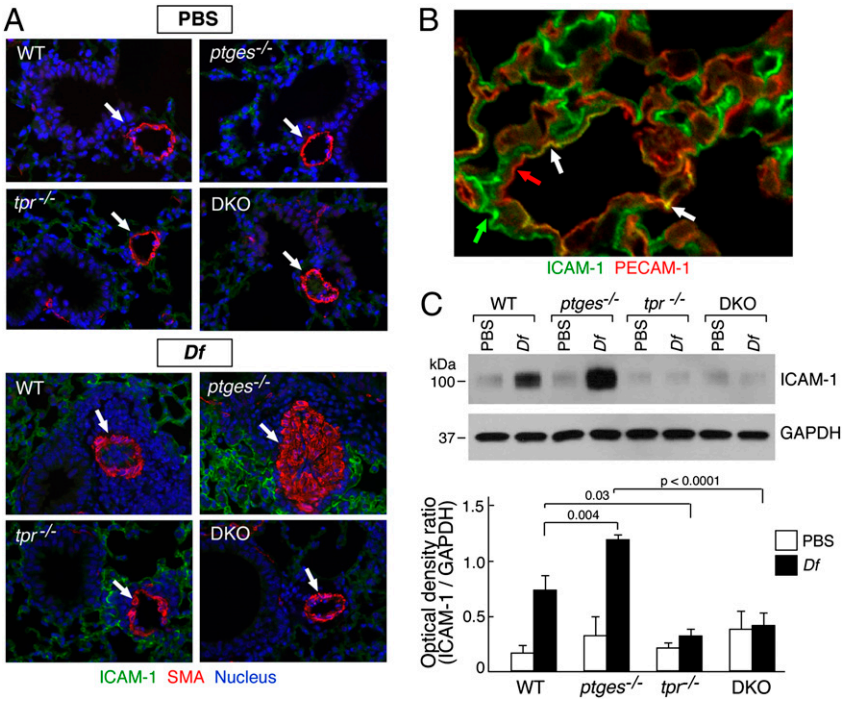

Fig. 5. PGE_2 deficiency amplifies the contribution of TP-dependent ICAM-1 induction. (*A*) Double immunofluorescent stains of bronchovascular bundles in the lungs of saline (*Upper*) and *Df*-challenged mice of the indicated genotypes. Paraffin-embedded lung sections were stained for α-SMA (red fluorescence, to identify pulmonary arterioles, as indicated by arrows) and ICAM-1 (green fluorescence), and counterstained with Hoechst stain to detect the nuclei (blue). Note that ICAM-1 localizing primarily to alveolar walls. Images are 400×. (*B*) Confocal imaging (1,200×) of the lung of a *Df*-challenged *ptges*$^{-/-}$ mouse double-stained for ICAM-1 (green fluorescence) and the endothelial cell marker PECAM-1 (red fluorescence). ICAM-1 localizes to PECAM-1^{-} alveolar epithelial cells (white arrowhead), and to PECAM-1^{+} endothelial cells (white arrows). Some additional PECAM-1^{+} cells are negative for ICAM-1 (red arrow). (*C*) Western blot of proteins extracted from the lungs of the indicated strains showing inducible expression of ICAM-1 with *Df* treatment and the effect of TP receptor deletion. Results are shown for representative mice (*Upper*), and densitometry is shown for groups of five to seven mice (*Lower*).

Consequently, TP-dependent effects become magnified in the setting of inflammation if the capacity to up-regulate PGE_2 generation (or to signal through EP receptors) is impaired. Deficient PGE_2 may potentiate AHR in the setting of eosinophilic inflammation (15, 47). Defective COX-2–dependent production of PGE_2 and deficient expression of EP_2 receptors have both been documented in AERD (19, 21, 48), and might account for the marked eosinophilic airway inflammation and high basal levels of leukotriene E_4 typical of this syndrome. The lack of a contribution from COX-2 to the generation of homeostatic PGE_2 may explain the fact that COX-2–selective agonists are well-tolerated in AERD (49). Because aspirin potently inhibits COX-1 but only weakly inhibits COX-2 (50), most asthmatic individuals likely tolerate aspirin because of the persistent bronchoprotection provided by "aspirin resistant" COX-2/mPGES-1–derived PGE_2. Conversely, the inability to maintain COX-2/mPGES-1–derived PGE_2 when COX-1 is inhibited could explain the characteristic surge in cysteinyl leukotriene production and bronchoconstriction in response to challenges with low-dose (30–160 mg) aspirin in individuals with AERD. Basal COX-1–derived TXA_2 formation is unimpaired in AERD (45). Subsequently, the interference with TXA_2 generation (51) could explain part of the apparently paradoxical therapeutic benefit of aspirin treatment in patients with AERD after they are clinically desensitized (52). Existing orally active TP receptor agonists have shown moderate efficacy in reducing AHR or sputum eosinophilia in small controlled studies of individuals with asthma (53–55). Such antagonists may have major efficacy as treatments for asthma in individuals stratified for lower levels of pulmonary PGE_2 production or deficient EP receptor signaling, such as those with AERD (21).

Methods

Mice. C57BL/6 *ptges*$^{-/-}$ mice were from Satoshi Uematsu (Osaka University, Osaka, Japan). C57BL/6 *tpr*$^{-/-}$ mice were provided by Thomas Coffman (Duke University, Durham, NC). *ptges*$^{-/-}$ males were intercrossed with *tpr*$^{-/-}$ females to obtain double-KO (*ptges*/*tpr*$^{-/-}$) mice. The mice and the WT controls were housed at Charles River. All studies were conducted on 6- to 8-wk-old male mice and were approved by the Animal Care and Use Committee of the Dana-Farber Cancer Institute. *Df* challenges, cellular and standard histologic analyses, restimulation of PLN cells, measurements of Abs, and GC-MS analyses were all performed as described previously (12, 56).

Bone Marrow Transfer. Five-week-old mice were lethally irradiated with 1,200 rads (12 Gy) in two split doses, 4 h apart. Within 24 h of irradiation, 1×10^7 bone marrow cells were infused via the tail vein into sex-matched irradiated mice in 200 μL of PBS. For the first 8 wk after the injection of bone marrow cells, chimeric mice drank water supplemented with enrofloxacin (Baytril; Bayer Health Care). Ten weeks after the injection, mice were exposed to six doses of saline or *Df* and killed 24 h after the last challenge. Peripheral blood cell counts were performed before the beginning of treatment to ensure full engraftment.

ICAM-1 Blocking. Twenty-four hours before each *Df* challenge, mice were injected intraperitoneally with 50 μg of a neutralizing Ab against mouse ICAM-1 (clone YN1/1.7.4; Biolegend) or rat IgG2b-κ isotype control Ab (Biolegend). Mice were treated with 3 μg of *Df* twice weekly for 3 wk.

Statistical Analysis. Data are expressed as mean ± SD. Statistical analyses were performed using ANOVA. Differences were considered significant when *P* values were less than 0.05.

ACKNOWLEDGMENTS. This work was supported by National Institutes of Health Grants AI 052353, AT 002782, AI095219, and AI078908 and by generous contributions from the Vinik Family.

1. Smyth EM, Grosser T, Wang M, Yu Y, FitzGerald GA (2009) Prostanoids in health and disease. *J Lipid Res* 50(Suppl):S423–S428.
2. Kobayashi T, Narumiya S (2002) Function of prostanoid receptors: Studies on knockout mice. *Prostaglandins Other Lipid Mediat* 68-69:557–573.
3. Emery P, Koncz T, Pan S, Lowry S (2008) Analgesic effectiveness of celecoxib and diclofenac in patients with osteoarthritis of the hip requiring joint replacement surgery: A 12-week, multicenter, randomized, double-blind, parallel-group, double-dummy, noninferiority study. *Clin Ther* 30:70–83.
4. Rahme E, Bernatsky S (2010) NSAIDs and risk of lower gastrointestinal bleeding. *Lancet* 376:146–148.
5. Matsumoto H, et al. (1997) Concordant induction of prostaglandin E2 synthase with cyclooxygenase-2 leads to preferred production of prostaglandin E2 over thromboxane and prostaglandin D2 in lipopolysaccharide-stimulated rat peritoneal macrophages. *Biochem Biophys Res Commun* 230:110–114.
6. Murakami M, et al. (2003) Cellular prostaglandin E2 production by membrane-bound prostaglandin E synthase-2 via both cyclooxygenases-1 and -2. *J Biol Chem* 278: 37937–37947.
7. Tanioka T, Nakatani Y, Semmyo N, Murakami M, Kudo I (2000) Molecular identification of cytosolic prostaglandin E2 synthase that is functionally coupled with cyclooxygenase-1 in immediate prostaglandin E2 biosynthesis. *J Biol Chem* 275: 32775–32782.
8. Uematsu S, Matsumoto M, Takeda K, Akira S (2002) Lipopolysaccharide-dependent prostaglandin E(2) production is regulated by the glutathione-dependent prostaglandin E(2) synthase gene induced by the Toll-like receptor 4/MyD88/NF-IL6 pathway. *J Immunol* 168:5811–5816.
9. Sugimoto Y, Narumiya S (2007) Prostaglandin E receptors. *J Biol Chem* 282: 11613–11617.
10. Yao C, et al. (2009) Prostaglandin E2-EP4 signaling promotes immune inflammation through Th1 cell differentiation and Th17 cell expansion. *Nat Med* 15:633–640.
11. Hartney JM, et al. (2006) Prostaglandin E2 protects lower airways against bronchoconstriction. *Am J Physiol Lung Cell Mol Physiol* 290:L105–L113.
12. Lundequist A, et al. (2010) Prostaglandin E(2) exerts homeostatic regulation of pulmonary vascular remodeling in allergic airway inflammation. *J Immunol* 184:433–441.
13. Martin JG, et al. (2002) The immunomodulatory actions of prostaglandin E2 on allergic airway responses in the rat. *J Immunol* 169:3963–3969.
14. Gauvreau GM, Watson RM, O'Byrne PM (1999) Protective effects of inhaled PGE2 on allergen-induced airway responses and airway inflammation. *Am J Respir Crit Care Med* 159:31–36.
15. Sastre B, et al. (2008) Increased prostaglandin E2 levels in the airway of patients with eosinophilic bronchitis. *Allergy* 63:58–66.
16. Picado C, et al. (1999) Cyclooxygenase-2 mRNA is downexpressed in nasal polyps from aspirin-sensitive asthmatics. *Am J Respir Crit Care Med* 160:291–296.
17. Roca-Ferrer J, et al. (2011) Reduced expression of COXs and production of prostaglandin E(2) in patients with nasal polyps with or without asperin-intolerant asthma. *J Allergy Clin Immunol* 128:66–72.e1.
18. Yoshimura T, Yoshikawa M, Otori N, Haruna S, Moriyama H (2008) Correlation between the prostaglandin D(2)/E(2) ratio in nasal polyps and the recalcitrant pathophysiology of chronic rhinosinusitis associated with bronchial asthma. *Allergol Int* 57:429–436.
19. Pierzchalska M, Szabó Z, Sanak M, Soja J, Szczeklik A (2003) Deficient prostaglandin E2 production by bronchial fibroblasts of asthmatic patients, with special reference to aspirin-induced asthma. *J Allergy Clin Immunol* 111:1041–1048.
20. Corrigan CJ, et al. (2012) Reduced expression of the prostaglandin E(2) receptor E-prostanoid 2 on bronchial mucosal leukocytes in patients with aspirin-sensitive asthma. *J Allergy Clin Immunol* 129:1636–1646.
21. Ying S, et al. (2006) Aspirin-sensitive rhinosinusitis is associated with reduced E-prostanoid 2 receptor expression on nasal mucosal inflammatory cells. *J Allergy Clin Immunol* 117:312–318.
22. Barrett NA, et al. (2011) Dectin-2 mediates Th2 immunity through the generation of cysteinyl leukotrienes. *J Exp Med* 208:593–604.
23. Daley E, et al. (2008) Pulmonary arterial remodeling induced by a Th2 immune response. *J Exp Med* 205:361–372.
24. Zarbock A, Singbartl K, Ley K (2006) Complete reversal of acid-induced acute lung injury by blocking of platelet-neutrophil aggregation. *J Clin Invest* 116:3211–3219.
25. Jankov RP, et al. (2002) Thromboxane A(2) receptors mediate pulmonary hypertension in 60% oxygen-exposed newborn rats by a cyclooxygenase-independent mechanism. *Am J Respir Crit Care Med* 166:208–214.
26. Grosser T, et al. (1997) Thromboxane A2 induces cell signaling but requires platelet-derived growth factor to act as a mitogen. *Eur J Pharmacol* 319:327–332.
27. Jones GL, Saroea HG, Watson RM, O'Byrne PM (1992) Effect of an inhaled thromboxane mimetic (U46619) on airway function in human subjects. *Am Rev Respir Dis* 145:1270–1274.
28. Thomas DW, Coffman TM (1998) A genetic approach for studying the role of thromboxane A2 in the kidney. *Kidney Int Suppl* 67:S84–S87.
29. Rydell-Törmänen K, Johnson JR, Fattouh R, Jordana M, Erjefält JS (2008) Induction of vascular remodeling in the lung by chronic house dust mite exposure. *Am J Respir Cell Mol Biol* 39:61–67.
30. Allen IC, et al. (2006) Thromboxane A2 induces airway constriction through an M3 muscarinic acetylcholine receptor-dependent mechanism. *Am J Physiol Lung Cell Mol Physiol* 290:L526–L533.
31. Church RJ, Jania LA, Koller BH (2012) Prostaglandin E2 produced by the lung augments the effector phase of allergic inflammation. *J Immunol* 188:4093–4102.
32. Venkayya R, et al. (2002) The Th2 lymphocyte products IL-4 and IL-13 rapidly induce airway hyperresponsiveness through direct effects on resident airway cells. *Am J Respir Cell Mol Biol* 26:202–208.
33. Kabashima K, et al. (2003) Thromboxane A2 modulates interaction of dendritic cells and T cells and regulates acquired immunity. *Nat Immunol* 4:694–701.
34. Nagamachi M, et al. (2007) Facilitation of Th1-mediated immune response by prostaglandin E receptor EP1. *J Exp Med* 204:2865–2874.
35. Boulet L, et al. (2004) Deletion of microsomal prostaglandin E2 (PGE2) synthase-1 reduces inducible and basal PGE2 production and alters the gastric prostanoid profile. *J Biol Chem* 279:23229–23237.
36. Wang M, et al. (2006) Deletion of microsomal prostaglandin E synthase-1 augments prostacyclin and retards atherogenesis. *Proc Natl Acad Sci USA* 103:14507–14512.
37. Hinton M, Gutsol A, Dakshinamurti S (2007) Thromboxane hypersensitivity in hypoxic pulmonary artery myocytes: Altered TP receptor localization and kinetics. *Am J Physiol Lung Cell Mol Physiol* 292:L654–L663.
38. Santhosh KT, et al. (2011) Milrinone attenuates thromboxane receptor-mediated hyperresponsiveness in hypoxic pulmonary arterial myocytes. *Br J Pharmacol* 163: 1223–1236.
39. Kunikata T, et al. (2005) Suppression of allergic inflammation by the prostaglandin E receptor subtype EP3. *Nat Immunol* 6:524–531.
40. Kobayashi K, Murata T, Hori M, Ozaki H (2011) Prostaglandin E2-prostanoid EP3 signal induces vascular contraction via nPKC and ROCK activation in rat mesenteric artery. *Eur J Pharmacol* 660:375–380.
41. Walsh MT, Kinsella BT (2000) Regulation of the human prostanoid TPalpha and TPbeta receptor isoforms mediated through activation of the EP(1) and IP receptors. *Br J Pharmacol* 131:601–609.
42. Iyu D, et al. (2011) PGE(1) and PGE(2) modify platelet function through different prostanoid receptors. *Prostaglandins Other Lipid Mediat* 94(1–2):9–16.
43. Ishizuka T, et al. (1998) Stimulation with thromboxane A2 (TXA2) receptor agonist enhances ICAM-1, VCAM-1 or ELAM-1 expression by human vascular endothelial cells. *Clin Exp Immunol* 112:464–470.
44. Pitchford SC, et al. (2005) Platelet P-selectin is required for pulmonary eosinophil and lymphocyte recruitment in a murine model of allergic inflammation. *Blood* 105: 2074–2081.
45. Laidlaw TM, et al. (2012) Cysteinyl leukotriene overproduction in aspirin-exacerbated respiratory disease is driven by platelet-adherent leukocytes. *Blood* 119:3790–3798.
46. Tilley SL, et al. (2003) Receptors and pathways mediating the effects of prostaglandin E2 on airway tone. *Am J Physiol Lung Cell Mol Physiol* 284:L599–L606.
47. Aggarwal S, Moodley YP, Thompson PJ, Misso NL (2010) Prostaglandin E2 and cysteinyl leukotriene concentrations in sputum: association with asthma severity and eosinophilic inflammation. *Clin Exp Allergy* 40:85–93.
48. Kowalski ML, et al. (2000) Differential metabolism of arachidonic acid in nasal polyp epithelial cells cultured from aspirin-sensitive and aspirin-tolerant patients. *Am J Respir Crit Care Med* 161:391–398.
49. Woessner KM, Simon RA, Stevenson DD (2002) The safety of celecoxib in patients with aspirin-sensitive asthma. *Arthritis Rheum* 46:2201–2206.
50. Smith WL, Meade EA, Dewitt DL (1997) Interaction of PGH synthase isozymes-1 and -2 with nonsteroidal anti-inflammatory drugs. *Adv Exp Med Biol* 400A:189–196.
51. Sladek K, Szczeklik A (1993) Cysteinyl leukotrienes overproduction and mast cell activation in aspirin-provoked bronchospasm in asthma. *Eur Respir J* 6:391–399.
52. Berges-Gimeno MP, Simon RA, Stevenson DD (2003) Early effects of aspirin desensitization treatment in asthmatic patients with aspirin-exacerbated respiratory disease. *Ann Allergy Asthma Immunol* 90:338–341.
53. Aizawa H, et al. (1998) Effects of thromboxane A2 antagonist on airway hyperresponsiveness, exhaled nitric oxide, and induced sputum eosinophils in asthmatics. *Prostaglandins Leukot Essent Fatty Acids* 59:185–190.
54. Aizawa H, Shigyo M, Nogami H, Hirose T, Hara N (1996) BAY u3405, a thromboxane A2 antagonist, reduces bronchial hyperresponsiveness in asthmatics. *Chest* 109: 338–342.
55. Hoshino M, Sim J, Shimizu K, Nakayama H, Koya A (1999) Effect of AA-2414, a thromboxane A2 receptor antagonist, on airway inflammation in subjects with asthma. *J Allergy Clin Immunol* 103:1054–1061.
56. Giannattasio G, et al. (2011) The purinergic G protein-coupled receptor 6 inhibits effector T cell activation in allergic pulmonary inflammation. *J Immunol* 187: 1486–1495.

Supporting Information

Liu et al. 10.1073/pnas.1207816109

SI Methods

Reagents. Mice were treated with PBS or *Df*, an extract of the house dust mite *Dermatophagoides farina,* from Greer Laboratories (XPB81D3A25; containing <0.005 EU/mL of endotoxin) dissolved in PBS. Selective agonists of the E prostanoid $(EP)_1$ (DI-004), EP_2 (AE1-259-01), EP_3 (AE-248), and EP_4 (AE-329) receptors were from Ono Pharmaceuticals. The selective T prostanoid (TP) receptor agonist U-46619 and the TP receptor antagonist SQ 29,548 were from Cayman Chemical. Selective inhibitors of PKA (H89) and PKC (Go6976, Calphostin C) were from Sigma.

Immunofluorescence. Direct immunofluorescence was performed on paraffin-embedded specimens with Alexa Fluor 488 labeled anti-mouse CD54 (intercellular adhesion molecule-1, ICAM-1) for ICAM-1 and Cy3 conjugated monoclonal anti–α-smooth muscle actin (α-SMA) (Sigma-Aldrich). Sections were blocked for 30 min with 10% donkey serum in PBS and then incubated with the Abs (diluted 1:200 for anti–ICAM-1 and 1:500 for α-SMA in PBS containing 1% BSA) for 60 min. Sections were washed in PBS, counterstained with Hoechst 33342 (Sigma; 2.5 μg/mL) for nuclear staining, and mounted with aqueous antiquenching medium. Microscopy and photography were performed with a Leica DMRXA microscope.

Double indirect immunofluorescence was performed with unlabeled goat anti-mouse platelet endothelial adhesion molecule-1 (PECAM-1; R&D Systems) and rat anti-mouse CD54 (Biolegend). After blocking, sections were incubated with the Abs (diluted 1:200 for PECAM-1 anti–ICAM-1 and 1:100 for ICAM-1 in PBS containing 1% BSA) at 4 °C overnight. The washed sections were incubated with Alexa 594 chicken anti-goat IgG and Alexa 488 donkey anti-rat IgG (both from Invitrogen) at room temperature for 60 min, and then washed again. The sections were mounted with SlowFade Gold reagent with Dabi (Invitrogen). Microscopy and photography were performed with a Nikon 80 Microscope Air and Nikon TE2000-U inverted Microscope equipped with a C1Plus confocal system.

Flow Cytometry. Whole heparinized blood was stimulated with various doses of the TP receptor agonist U-46619 for 15 min. Some samples were pretreated for 20 min with various EP receptor agonists immediately after 30 min of treatment with PKC or PKA inhibitors for 30 min. The samples were stained with FITC-conjugated anti-CD41 and phycoerythrin (PE)-conjugated CD62P Abs or corresponding isotype controls for 1 h at 4 °C, and fixed in 1% paraformaldehyde. The data were acquired on a FACS Canto flow cytometer with FACA Diva software (BD Biosciences), and analyzed with FlowJo (Tree Star).

Human umbilical vein endothelial cells were incubated with various concentrations of PKA or PKC inhibitors for 30 min, then with various concentrations of EP agonists for 30 min, and then with various concentration of U-46119 for 24 h. Then the cells were incubated with PE-conjugated anti–ICAM-1 (Biolegend), or isotype controls for 1 h at 4 °C and fixed in 1% paraformaldehyde.

Western Blot. Lungs were homogenized at 4 °C in the presence of T-PER Plus Halt Protease Inhibitor Mixture Kit (Pierce). Total protein concentrations in the lung tissue homogenates were determined using a BCA Protein Assay Kit (Pierce). Protein (30 μg) was electrophoresed on 10% polyacrylamide gels and blotted onto PVDF membrane (GE Healthcare). Western blotting was performed with a goat anti-mouse ICAM-1 Ab (R&D Systems).

Measurement of Airway Hyperresponsiveness to Methacholine. Changes in lung resistance induced by methacholine (MCh) were measured with the Buxco invasive measurement system (Buxco) 24 h after the last *Df* challenge. Mice were anesthetized with 90 mg/kg body weight of intraperitoneal pentobarbital. Tracheas were connected with a ventilator (MiniVent 845; Harvard Apparatus) via a 19-gauge needle. The mice were ventilated at a frequency of 150 breaths per minute with 200-μL stroke volume. Aerosolized saline and increasing concentrations of MCh (dissolved in saline at 6.25, 12.5, 25, 50, and 100 mg/mL) were administered. Airflow and pressure changes were recorded with Bio System XA software (Buxco). Airway hyperresponsiveness is expressed as percentage change from the baseline level of lung resistance.

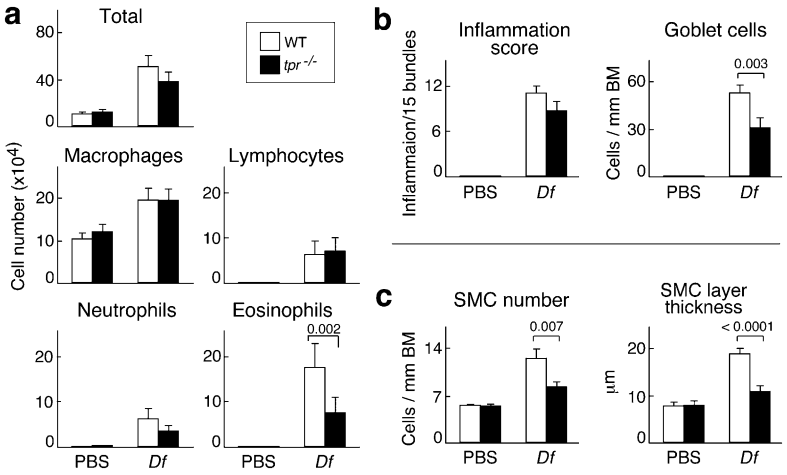

Fig. S1. Deletion of TP receptors reduces inflammation in PGE_2-sufficient mice challenged with high dose *Df*. Mice were challenged intranasally on six occasions with 10 μg *Df*. (*A*) Total cell counts and differential cell counts are shown for the bronchoalveolar lavage (BAL) fluid from the indicated genotypes. (*B*) Quantitation of bronchovascular inflammation and goblet cell counts from the lungs of the indicated genotypes. (*C*) Quantitation of α-SMA$^+$ cell numbers and thickness of the α-SMA$^+$ vascular wall in saline- and *Df*-challenged mice from the indicated genotypes. The results in *A*–*C* are from 18 to 23 mice per group in four separate experiments.

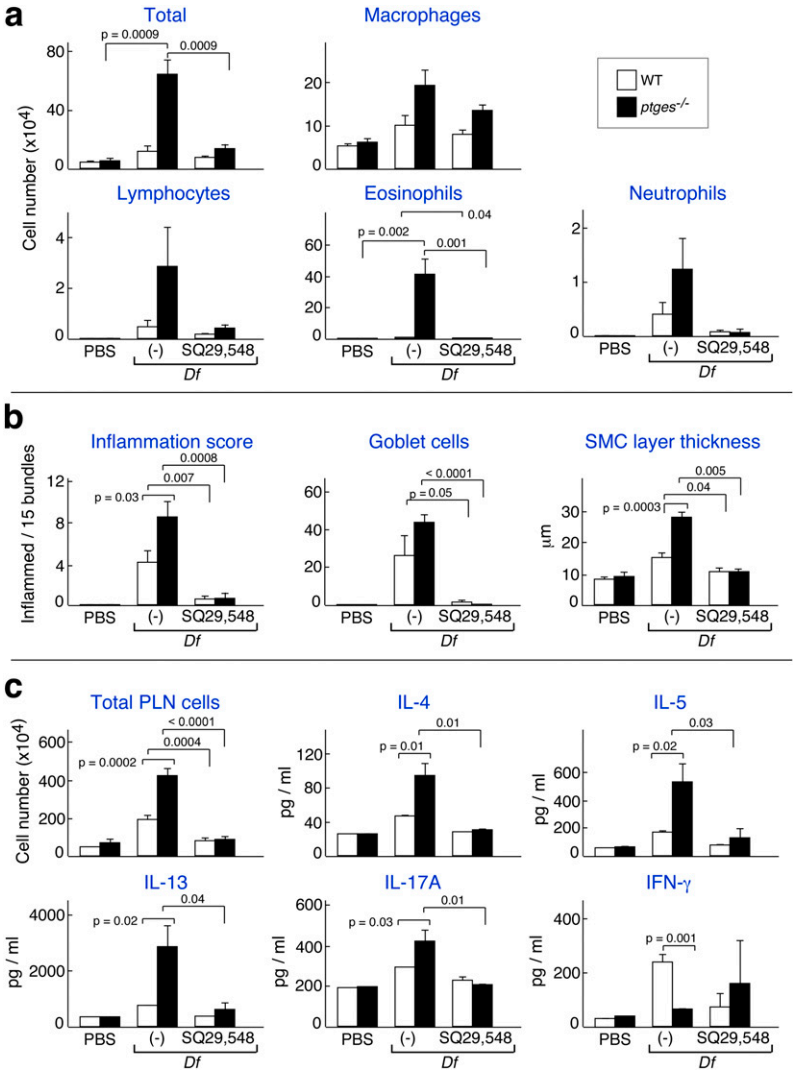

Fig. S2. Treatment with a TP receptor antagonist reduces *Df*-induced inflammation and cytokine production. Mice from the indicated genotypes were treated intraperitoneally on a daily basis with the selective TP receptor antagonist SQ 29,548 during the period of intranasal *Df* or saline challenge. (*A*) BAL fluid cell counts and differentials; (*B*) Quantitative assessments of bronchovascular inflammation and goblet cells; (*C*) and cytokine generation by restimulated parabronchial lymph node (PLN) cells. Results are from five mice per group.

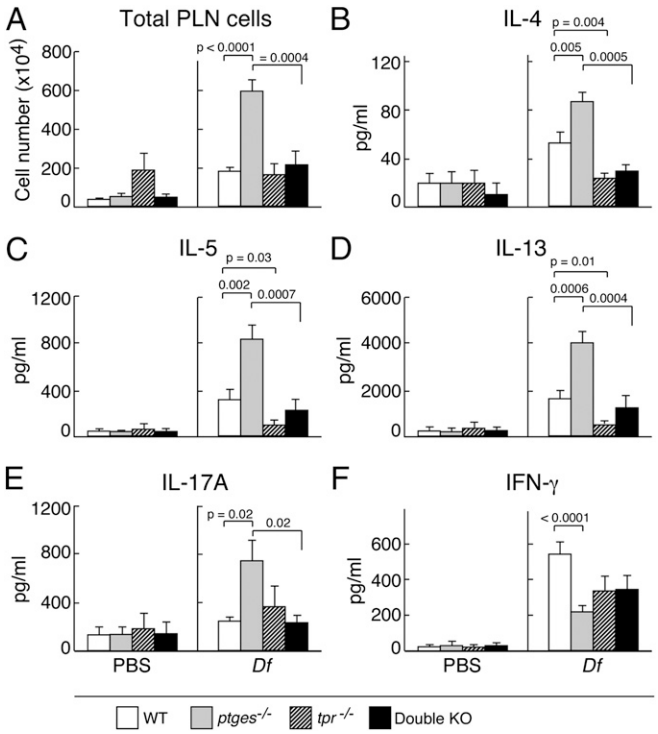

Fig. S3. Deletion of TP receptors attenuates effector cytokine generation by restimulated PLN cells. PLNs were removed from the thoracic cavities of saline- or *Df*-challenged mice 24 h after the last challenge. Cells were dispersed and counted, and 2.5×10^5 PLN cells were plated and restimulated for 72 h with *Df*. (*A*) Total PLN cells recovered from saline- or *Df*-challenged mice of the indicated genotypes. (*B–F*) Cytokine production by the restimulated PLN cells as measured by ELISA. Data are mean ± SD from 10 to 15 mice per group from three separate experiments.

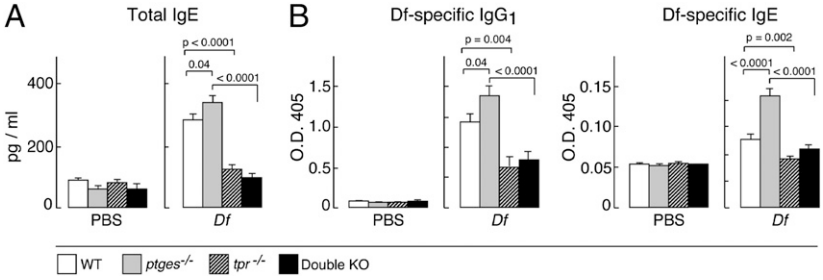

Fig. S4. Deletion of TP receptors attenuates the systemic production of IgE and specific IgG1. Serum was obtained from mice of the indicated genotypes after challenge with saline or *Df*. Total IgE (*A*) and *Df*-specific IgG_1 and IgE (*B*) were measured by ELISA. Data are mean ± SD from 10 mice per group from two different experiments.

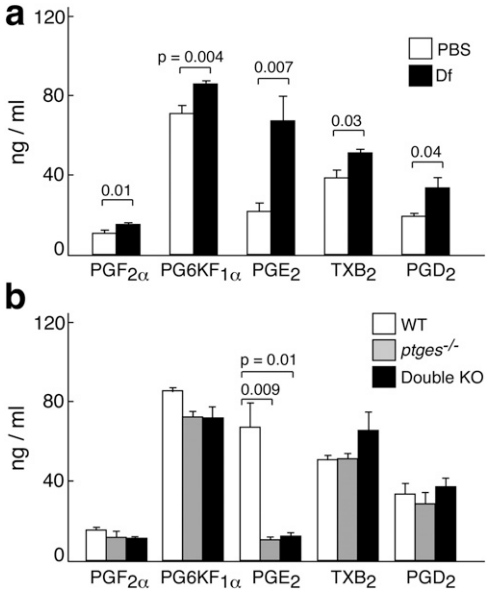

Fig. S5. *Df*-induced pulmonary inflammation selectively up-regulates microsomal prostaglandin E_2 synthase (mPGES)-1–dependent prostaglandin E_2 (PGE_2)-producing capability of lung cells. The lungs were removed from *Df*- or saline-challenged mice and mechanically dispersed. The conversion of exogenous arachidonic acid to various PGs was monitored by GC-MS. (*A*) Effect of *Df* on conversion of arachidonic acid to PGs by the lung cells from WT mice. (*B*) Effect of *ptges* or *tpr* deletions on the conversion of arachidonic acid to PGs by the lungs of *Df*-challenged mice. Data are mean ± SD from four to five mice per group from a single experiment. Results in a second experiment were similar.

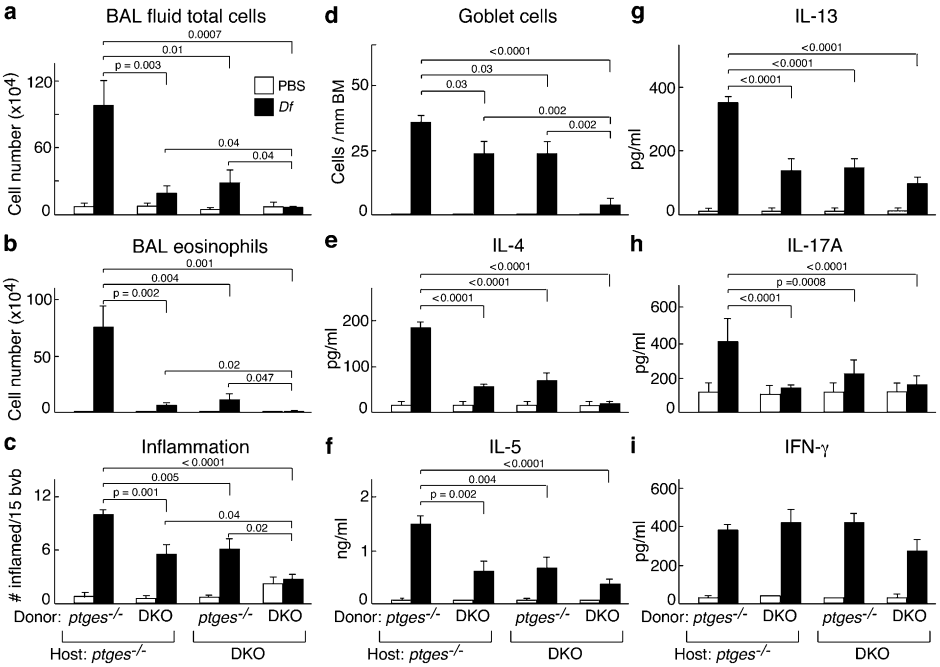

Fig. S6. TP receptors on both hematopoietic and resident lung cells contribute to the phenotype of PGE_2 deficiency. Lethally irradiated $ptges^{-/-}$ and double-KO (DKO) mice received transfers of 1×10^7 bone marrow cells from mice of the indicated genotypes. Ten weeks later, the mice were challenged with saline or *Df* on six occasions and were killed after the last challenge. (*A*) Total BAL fluid cell counts and (*B*) total BAL fluid eosinophil counts recovered from the indicated groups. (*C*) Analysis of inflammation, (*D*) goblet cell metaplasia, and (*E–I*) cytokine generation by restimulated PLN cells. Data are mean ± SD from 10 mice per group from two separate experiments.

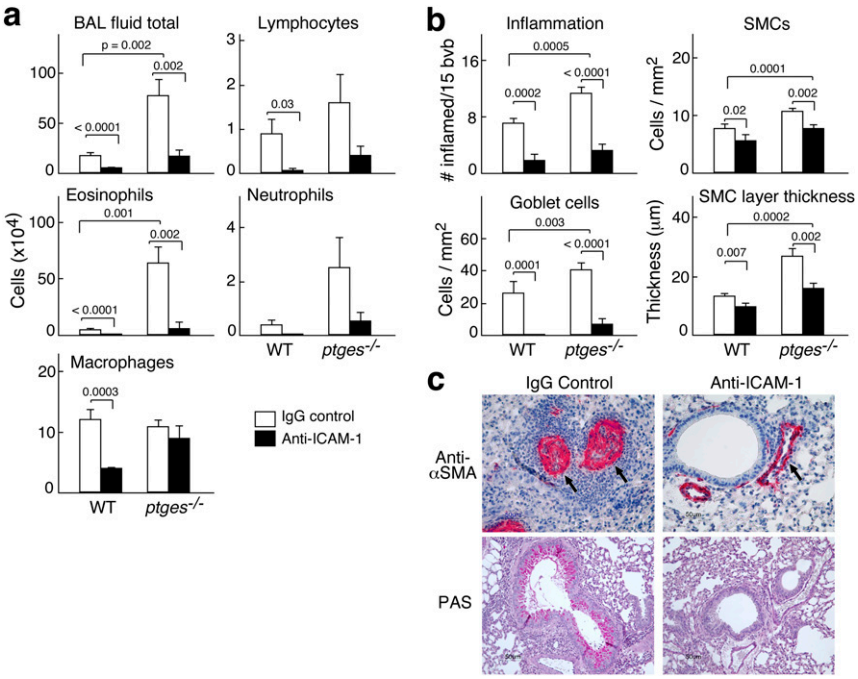

Fig. S7. Effect of intraperitoneal administration of anti–ICAM-1 monoclonal Abs on *Df*-induced pulmonary inflammation. (*A*) BAL fluid total cell count and differential cell counts in *Df*-challenged WT and *ptges*$^{-/-}$ mice treated with anti–ICAM-1 Ab or IgG control. (*B*) Bronchovascular bundle inflammation, goblet cell counts, and arteriolar smooth muscle cell (SMC) layer thickness and numbers in *Df*-challenged WT and *ptges*$^{-/-}$ mice treated with the Abs. (*C*) Representative micrographs of lungs from *Df*-challenged *ptges*$^{-/-}$ mice treated with the indicated Abs showing immunostains for α-SMA (*Upper*) to indicate arterioles (arrows), and Periodic acid-Schiff (PAS) stains (*Lower*) to illustrate goblet cells. Results in *A* and *B* are the mean ± SD from 10 mice per group in two independent experiments.

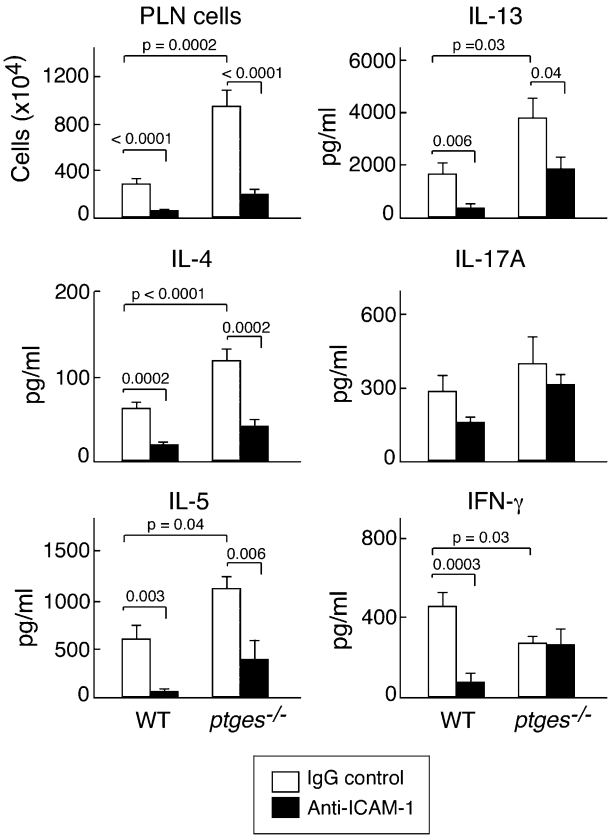

Fig. S8. Effect of ICAM-1 blockade on PLN cell counts and cytokine generation with *Df* restimulation. Cell counts from PLNs harvested from *Df*-challenged mice of the indicated strains treated with either anti–ICAM-1 Abs or with isotype control Abs. Cytokine generation by PLN cells (2.5×10^5/sample) from the same groups after 72 h of restimulation with *Df*. Data in *B* are from 10 mice per group from two independent experiments.